An underwater photograph of a coral reef. The water is a deep blue. In the foreground, there are large, dense patches of coral that appear bleached, showing a pale yellowish-white color. To the right, there are more complex, branching coral structures that are darker, possibly brown or black, indicating they may be dead or severely damaged. The background shows more coral and the water surface with some light reflections.

EXPLAINING EXTREME EVENTS OF 2016

From A Climate Perspective

Special Supplement to the
Bulletin of the American Meteorological Society
Vol. 99, No. 1, January 2018

EXPLAINING EXTREME EVENTS OF 2016 FROM A CLIMATE PERSPECTIVE

Editors

Stephanie C. Herring, Nikolaos Christidis, Andrew Hoell, James P. Kossin,
Carl J. Schreck III, and Peter A. Stott

Special Supplement to the

Bulletin of the American Meteorological Society

Vol. 99, No. 1, January 2018

AMERICAN METEOROLOGICAL SOCIETY

CORRESPONDING EDITOR:

Stephanie C. Herring, PhD
NOAA National Centers for Environmental Information
325 Broadway, E/CC23, Rm 1B-131
Boulder, CO 80305-3328
E-mail: stephanie.herring@noaa.gov

COVER CREDIT:

©The Ocean Agency / XL Catlin Seaview Survey / Christophe Bailhache—A panoramic image of coral bleaching at Lizard Island on the Great Barrier Reef, captured by The Ocean Agency / XL Catlin Seaview Survey / Christophe Bailhache in March 2016.

HOW TO CITE THIS DOCUMENT

Citing the complete report:

Herring, S. C., N. Christidis, A. Hoell, J. P. Kossin, C. J. Schreck III, and P. A. Stott, Eds., 2018: Explaining Extreme Events of 2016 from a Climate Perspective. *Bull. Amer. Meteor. Soc.*, **99** (1), SI–SI57.

Citing a section (example):

Quan, X.W., M. Hoerling, L. Smith, J. Perlwitz, T. Zhang, A. Hoell, K. Wolter, and J. Eischeid, 2018: Extreme California Rains During Winter 2015/16: A Change in El Niño Teleconnection? [in “Explaining Extreme Events of 2016 from a Climate Perspective”]. *Bull. Amer. Meteor. Soc.*, **99** (1), S54–S59, doi:10.1175/BAMS-D-17-0118.1.

EDITORIAL AND PRODUCTION TEAM

Riddle, Deborah B., Lead Graphics Production, NOAA/NESDIS National Centers for Environmental Information, Asheville, NC

Love-Brotak, S. Elizabeth, Graphics Support, NOAA/NESDIS National Centers for Environmental Information, Asheville, NC

Veasey, Sara W., Visual Communications Team Lead, NOAA/NESDIS National Centers for Environmental Information, Asheville, NC

Fulford, Jennifer, Editorial Support, Telesolv Consulting LLC, NOAA/NESDIS National Centers for Environmental Information, Asheville, NC

Griffin, Jessica, Graphics Support, Cooperative Institute for Climate and Satellites-NC, North Carolina State University, Asheville, NC

Misch, Deborah J., Graphics Support, Telesolv Consulting LLC, NOAA/NESDIS National Centers for Environmental Information, Asheville, NC

Osborne, Susan, Editorial Support, Telesolv Consulting LLC, NOAA/NESDIS National Centers for Environmental Information, Asheville, NC

Sprain, Mara, Editorial Support, LAC Group, NOAA/NESDIS National Centers for Environmental Information, Asheville, NC

Young, Teresa, Graphics Support, Telesolv Consulting LLC, NOAA/NESDIS National Centers for Environmental Information, Asheville, NC

TABLE OF CONTENTS

Abstract.....	ii
1. Introduction to Explaining Extreme Events of 2016 from a Climate Perspective	I
2. Explaining Extreme Ocean Conditions Impacting Living Marine Resources	7
3. CMIP5 Model-based Assessment of Anthropogenic Influence on Record Global Warmth During 2016.....	11
4. The Extreme 2015/16 El Niño, in the Context of Historical Climate Variability and Change	16
5. Ecological Impacts of the 2015/16 El Niño in the Central Equatorial Pacific	21
6. Forcing of Multiyear Extreme Ocean Temperatures that Impacted California Current Living Marine Resources in 2016	27
7. CMIP5 Model-based Assessment of Anthropogenic Influence on Highly Anomalous Arctic Warmth During November–December 2016.....	34
8. The High Latitude Marine Heat Wave of 2016 and Its Impacts on Alaska.....	39
9. Anthropogenic and Natural Influences on Record 2016 Marine Heat waves.....	44
10. Extreme California Rains During Winter 2015/16: A Change in El Niño Teleconnection?.....	49
11. Was the January 2016 Mid-Atlantic Snowstorm "Jonas" Symptomatic of Climate Change?...54	
12. Anthropogenic Forcings and Associated Changes in Fire Risk in Western North America and Australia During 2015/16.....	60
13. A Multimethod Attribution Analysis of the Prolonged Northeast Brazil Hydrometeorological Drought (2012–16).....	65
14. Attribution of Wintertime Anticyclonic Stagnation Contributing to Air Pollution in Western Europe.....	70
15. Analysis of the Exceptionally Warm December 2015 in France Using Flow Analogues.....	76
16. Warm Winter, Wet Spring, and an Extreme Response in Ecosystem Functioning on the Iberian Peninsula	80
17. Anthropogenic Intensification of Southern African Flash Droughts as Exemplified by the 2015/16 Season	86
18. Anthropogenic Enhancement of Moderate-to-Strong El Niño Events Likely Contributed to Drought and Poor Harvests in Southern Africa During 2016	91
19. Climate Change Increased the Likelihood of the 2016 Heat Extremes in Asia	97
20. Extreme Rainfall (R20mm, RX5day) in Yangtze–Huai, China, in June–July 2016: The Role of ENSO and Anthropogenic Climate Change.....	102
21. Attribution of the July 2016 Extreme Precipitation Event Over China's Wuhang	107
22. Do Climate Change and El Niño Increase Likelihood of Yangtze River Extreme Rainfall?....	113
23. Human Influence on the Record-breaking Cold Event in January of 2016 in Eastern China.....	118
24. Anthropogenic Influence on the Eastern China 2016 Super Cold Surge.....	123
25. The Hot and Dry April of 2016 in Thailand.....	128
26. The Effect of Increasing CO ₂ on the Extreme September 2016 Rainfall Across Southeastern Australia.....	133
27. Natural Variability Not Climate Change Drove the Record Wet Winter in Southeast Australia	139
28. A Multifactor Risk Analysis of the Record 2016 Great Barrier Reef Bleaching	144
29. Severe Frosts in Western Australia in September 2016.....	150
30. Future Challenges in Event Attribution Methodologies.....	155

This sixth edition of explaining extreme events of the previous year (2016) from a climate perspective is the first of these reports to find that some extreme events were not possible in a preindustrial climate. The events were the 2016 record global heat, the heat across Asia, as well as a marine heat wave off the coast of Alaska. While these results are novel, they were not unexpected. Climate attribution scientists have been predicting that eventually the influence of human-caused climate change would become sufficiently strong as to push events beyond the bounds of natural variability alone. It was also predicted that we would first observe this phenomenon for heat events where the climate change influence is most pronounced. Additional retrospective analysis will reveal if, in fact, these are the first events of their kind or were simply some of the first to be discovered.

Last year, the editors emphasized the need for additional papers in the area of “impacts attribution” that investigate whether climate change’s influence on the extreme event can subsequently be directly tied to a change in risk of the socio-economic or environmental impacts. Several papers in this year’s report address this challenge, including Great Barrier Reef bleaching, living marine resources in the Pacific, and ecosystem productivity on the Iberian Peninsula. This is an increase over the number of impact attribution papers than in the past, and are hopefully a sign that research in this area will continue to expand in the future.

Other extreme weather event types in this year’s edition include ocean heat waves, forest fires, snow storms, and frost, as well as heavy precipitation, drought, and extreme heat and cold events over land. There were

a number of marine heat waves examined in this year’s report, and all but one found a role for climate change in increasing the severity of the events. While human-caused climate change caused China’s cold winter to be less likely, it did not influence U.S. storm Jonas which hit the mid-Atlantic in winter 2016.

As in past years, the papers submitted to this report are selected prior to knowing the final results of whether human-caused climate change influenced the event. The editors have and will continue to support the publication of papers that find no role for human-caused climate change because of their scientific value in both assessing attribution methodologies and in enhancing our understanding of how climate change is, and is not, impacting extremes. In this report, twenty-one of the twenty-seven papers in this edition identified climate change as a significant driver of an event, while six did not. Of the 131 papers now examined in this report over the last six years, approximately 65% have identified a role for climate change, while about 35% have not found an appreciable effect.

Looking ahead, we hope to continue to see improvements in how we assess the influence of human-induced climate change on extremes and the continued inclusion of stakeholder needs to inform the growth of the field and how the results can be applied in decision making. While it represents a considerable challenge to provide robust results that are clearly communicated for stakeholders to use as part of their decision-making processes, these annual reports are increasingly showing their potential to help meet such growing needs.

23. HUMAN INFLUENCE ON THE RECORD-BREAKING COLD EVENT IN JANUARY OF 2016 IN EASTERN CHINA

CHENG QIAN, JUN WANG, SIYAN DONG, HONG YIN, CLAIRE BURKE,
ANDREW CIAVARELLA, BUWEN DONG, NICOLAS FREYCHET,
FRASER C. LOTT, AND SIMON F. B. TETT

Anthropogenic influences are estimated to have reduced the likelihood of an extreme cold event in midwinter with the intensity equal to or stronger than the record of 2016 in eastern China by about two-thirds.

Introduction. A strong cold surge occurred during 21–25 January 2016 affecting most areas of China, especially eastern China (Fig. 23.1a). Daily mean temperatures dropped by up to 10°C–18°C within this event at individual stations in this region (CMA 2017) and broke daily minimum temperature (T_{min}) records at many stations (Fig. 23.1b). The area averaged anomaly of T_{min} over the region (20°–44°N, 100°–124°E) for this pentad was –4°C (–2.2 standard deviations) relative to the 1961–90 normal. This was the lowest temperature recorded, for 21–25 January, since modern meteorological observations started in 1960 (Fig. 23.1c). According to press reports (CMA 2017), 1.18 billion people were in the area where daily mean temperatures fell by more than 6°C within this event. On 24 January, the snowline even reached Guangzhou and the Pearl River Delta in southern China. This was the lowest latitude recorded since 1951. A sharp temperature drop, low temperatures, and associated freezing rain and snow caused widespread disruptions to transport, power supply, and public services, and damage to agriculture

in southern China (<http://mt.sohu.com/20160210/n437184257.shtml>; last accessed 19 March 2017).

Cold extremes have been gaining wide attention in many parts of midlatitude Eurasia and North America in recent years (e.g., Mori et al. 2014; Trenary et al. 2016; McCusker et al. 2016). It is controversial whether they are related to Arctic warming. Some studies suggested that greenhouse-gas-induced global and Arctic warming may enhance the meandering of the jet stream thus increasing the probability of cold extremes in certain regions (Francis and Vavrus 2015), and that the Arctic warming in the Barents–Kara Seas is closely connected to the cooling in eastern Asia (Kug et al. 2015) and robust Arctic sea–ice influence on recent increases in Eurasian cold winters (Mori et al. 2014). However, other studies have suggested that the Arctic warming does not cause midlatitude cooling (e.g., McCusker et al. 2016; Sun et al. 2016).

Given the impact of this cold event in China and the controversy whether Asian midlatitude cold surges are becoming more likely as a consequence of Arctic warming, it is compelling to investigate how much anthropogenic forcing agents have affected the probability of cold events with an intensity equal to or larger than the January 2016 extreme event. We use the Met Office Hadley Centre system for attribution of extreme weather and climate events (ACE; Christidis et al. 2013; Burke and Stott 2017) and station observations to investigate the effect of anthropogenic forcings on the likelihood of such a cold event.

Data. We used observational data for T_{min} from 744 national Reference Climatic and Basic Meteorological Stations from the China National Meteorological Information Centre for the period 1960–2016. From 1960 to 2013, the updated temperature dataset

AFFILIATIONS: QIAN—CAS Key Laboratory of Regional Climate-Environment for Temperate East Asia, Institute of Atmospheric Physics, Chinese Academy of Sciences and University of Chinese Academy of Science, Beijing, China; WANG—CAS Key Laboratory of Regional Climate-Environment for Temperate East Asia, Institute of Atmospheric Physics, Chinese Academy of Sciences, Beijing, China; DONG, AND YIN—National Climate Center, China Meteorological Administration, Beijing, China; BURKE, CIAVARELLA, AND LOTT—Met Office Hadley Centre, Exeter, United Kingdom; DONG—National Centre for Atmospheric Science, Department of Meteorology, University of Reading, United Kingdom; FREYCHET, AND TETT—School of Geosciences, University of Edinburgh, Edinburgh, United Kingdom.

DOI:10.1175/BAMS-D-17-0095.1

A supplement to this article is available online (10.1175/BAMS-D-17-0095.2)

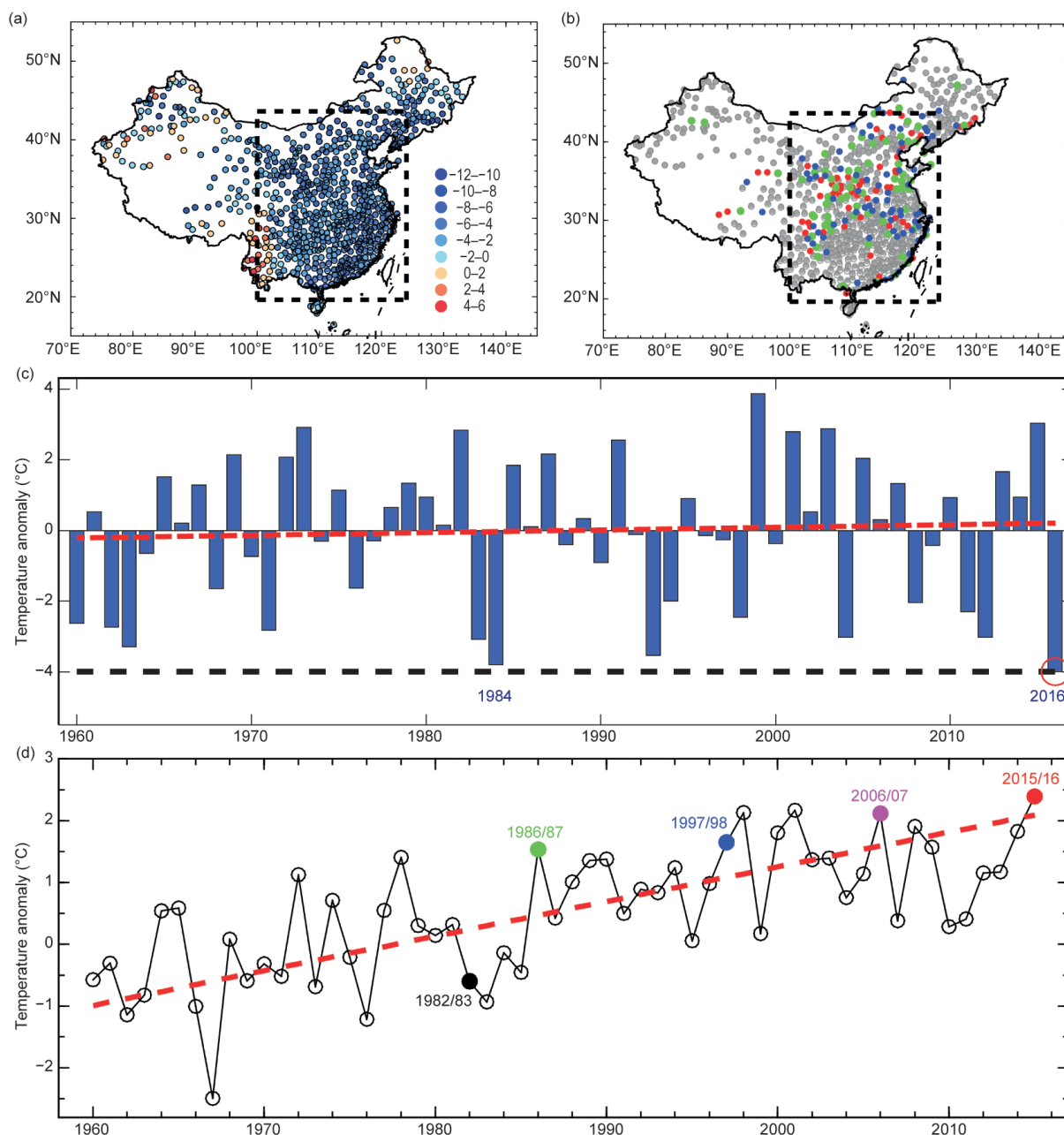


FIG. 23.1. (a) Observed pentad T_{min} anomalies (°C; relative to 1961–90 climatology) for 21–25 Jan 2016. Dashed box indicates study region (20°–44°N, 100°–124°E); (b) Colored dots represent stations that in 2016 recorded coldest (red), second coldest (green) and third coldest (blue) pentad T_{min} for any 21–25 Jan since 1960; (c) Time series of area-weighted average 21–25 pentad T_{min} anomaly °C over study region for 1960–2016. Red line shows linear trend of 0.078°C decade⁻¹; (d) Averaged winter T_{min} anomalies °C and corresponding linear trend over 1960/61–2015/16 in target region. Labeled dots show El Niño years

developed by Li et al. (2015) is used. This dataset was homogenized using the Multiple Analysis of Series for Homogenization (MASH) method (Szentimrey 1999) and was improved in terms of physical consistency among diurnal temperature records (Li et al. 2015), such that the temperature observations were quality-controlled and adjusted for most nonclimatic biases

due to the changes in the local observing system, such as station relocation. After 2013, it is updated directly from those stations that have continuous records to January 2016.

We used simulations of the Hadley Centre Global Environmental Model version 3 Global Atmosphere 6.0 (HadGEM3-GA6; Walters et al. 2017) at N216

resolution. Daily outputs of T_{min} at approximately $0.56^\circ \times 0.83^\circ$ horizontal resolution are used. Fifteen members of the historical (all forcing) 1961–90 period (histClim) are compared with observations to estimate the model bias. Two ensembles of 525 members with and without anthropogenic forcings are provided for January 2016 to estimate the risk of such a cold event. One of these ensembles (histALL) uses historical anthropogenic and natural forcings and is an extension of the previous 15-member histClim runs. The other ensemble (histNAT) uses natural forcings only and is a continuation of a historical natural ensemble of 15 members, complementary to the histClim runs. Beyond the initial conditions of this continuation, the only difference between each of the 525 members in these experiments is the stochastic physics seed, and they are therefore considered equivalent. The boundary conditions for the histNAT experiments (see online supplement) are the same as in previous experiments using an earlier version of Met Office attribution system (Christidis et al. 2013).

Methods. For each station, the observed daily T_{min} anomaly relative to 1961–90 was calculated, from which the pentad-mean T_{min} anomaly for 21–25 January (PT_{min}) of each year was computed. These PT_{min} were gridded into $2^\circ \times 2^\circ$ grid boxes for the region (20° – 44° N, 100° – 124° E) by simply averaging the available station data within a $2^\circ \times 2^\circ$ grid box. This region was chosen because the PT_{min} had a large negative anomaly in most stations of this region (Fig. 23.1a). We also calculated the regional average winter (December–February, DJF) T_{min} anomalies over the region.

To make observations and simulations comparable, the following steps were adopted: 1) For both histALL and histNAT ensembles, daily anomalies (relative to 1961–90 normal for histClim) were computed removing any constant model bias; 2) PT_{min} for 2016 in histALL and histNAT runs were calculated and a land–sea mask applied; 3) These masked anomalies were regridded to the same $2^\circ \times 2^\circ$ grid boxes as the observations using linear interpolation and masked by the observational gridded data; 4) Gridded observations were then masked by this simulated data; 5) The area-weighted average PT_{min} of both the observations (Fig. 23.1c) and the 525 histALL and histNAT runs were then computed.

To estimate the attributable risk (Stott et al. 2004, 2016) of such an extreme cold event in midwinter, area-weighted average T_{min} anomalies of 9 non-overlapping pentads from the coldest period in the

climatology (1 January to 15 February) from the 525 histALL and histNAT runs were calculated and fitted to probability distribution functions (PDFs). Goodness-of-fit was tested for Gaussian and generalized extreme value (GEV) distributions. The GEV fit was found to be the most appropriate (Fig. ES23.1) and return periods of an event like the one in 2016 were estimated from this GEV fit. The shape, scale, and location parameters of the GEV fit for histALL (histNAT) runs are -0.28 , 2.35 , and -0.21 (-0.31 , 2.25 , and -1.39), respectively.

Results. Figure 23.1a shows that during this extreme cold event, most stations in eastern China recorded negative PT_{min} , with the largest negative anomalies below -4°C . The PT_{min} broke the historical low temperature records for the same pentad at more than twenty stations, and many more recorded the second and third coldest pentad since 1960 (Fig. 23.1b). The linear trend in the regional average PT_{min} ($RAPT_{min}$; Fig. 23.1c) is $0.078^\circ\text{C decade}^{-1}$ with 95% confidence interval (-0.26 , 0.45), which is not statistically significant. This trend slope and significance testing is based on the nonparametric Sen's slope and Mann–Kendall test taking into account the first-order autocorrelation estimated by an iterative method (Wang and Swail 2001; WS2001). The 2016 $RAPT_{min}$ is the coldest 21–25 January in the record, which started 1960, beating the previous record in 1984 (Fig. 23.1c). Figure 23.1d shows that this cold event occurred in a background of the warmest winter T_{min} since 1960, showing a warming trend of 0.56 (-0.05 , 1.0054) $^\circ\text{C decade}^{-1}$ estimated also by WS2001, and that El Niño tends to be associated with warm winters (four-out-of-five El Niño years since 1982).

Figure 23.2a shows an overall mean shift toward warmer anomalies in histALL relative to histNAT indicating that human influences have reduced the risk of extreme cold events. To estimate the attributable risk ratio, we defined a threshold of -4°C based on the observed $RAPT_{min}$ for 2016. The probability (P_0) of an event equal to or colder than this threshold in midwinter in histNAT is 6.8%, whereas in histALL (P_1) it is only 2.3%. The risk ratio (P_1/P_0) is approximately 34%, which suggests that human influences have reduced the risk of such an extreme cold event by about 66%. We estimated the uncertainty of P_1/P_0 by resampling the PDF 1000 times (Pall et al. 2011). Results show that P_1/P_0 lies between 31.1% and 37.8% (one standard deviation), suggesting that human influences reduced the probability of such a cold event by approximately two

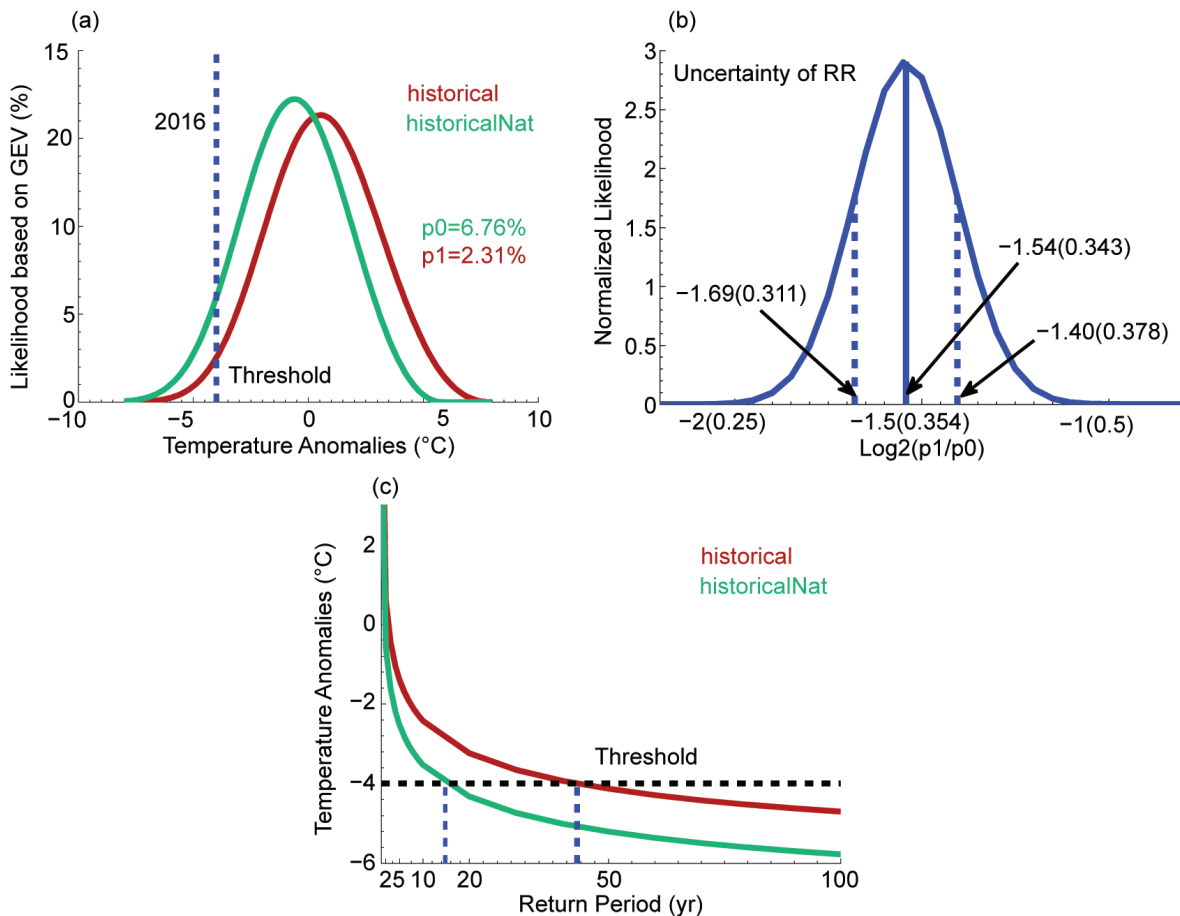


FIG. 23.2. (a) GEV distribution fit to 9×525 regional average pentad T_{min} anomalies $^{\circ}\text{C}$ during midwinter 2016 in eastern China from histALL simulations (red line; with anthropogenic and natural forcings) and that from histNAT simulations (green line; only with natural forcings). Dashed line indicates threshold, which is regional average pentad T_{min} anomaly of 21–25 Jan 2016 in observations. (b) Uncertainty in attributable risk ratio of such extreme cold event due to anthropogenic influences. Dashed lines indicate one standard deviation. (c) Return period (years) of extreme cold event with intensity equal or larger than extreme cold event of Jan 2016 in eastern China in histALL (red line) and histNAT simulations (green line). Black dashed line indicates threshold used in (a).

thirds (Fig. 23.2b). The estimated return period of RAPT_{min} like January 2016 is one-in-15 years with only natural forcings while it is extended to one-in-43 years with anthropogenic forcings (Fig. 23.2c).

Conclusions and discussion. Cold winters in China are expected to become rarer in a warming climate. By employing high quality station observations and model simulations, we estimate that anthropogenic influences have reduced the occurrence probability of an extreme cold event with the intensity equal to or stronger than the record in 2016 by approximately two-thirds. Conversely, if there were no anthropogenic influences, the probability of an extreme cold pentad in 2016 would be more than double. The return period of such a record cold event is estimated to have been extended by about 28 years due to human

influences. Our results are in line with McCusker et al. (2016) and Sun et al. (2016) and agree with Trenary et al. (2016) that despite severe cold surges and record-breaking extreme cold-day occurrences during 2016, winters have become warmer. Our results also imply that even under human-induced warming, extreme cold events can still occur as a result of natural variability, such as Arctic Oscillation, which was believed to be responsible for the reporting event (Cheung et al. 2016).

ACKNOWLEDGMENTS. We are grateful for the comments and suggestions provided by the editor and the reviewers. This study was largely carried out during a workshop on Operational Attribution at the University of Edinburgh sponsored by the U.K.–China Research & Innovation Partnership Fund through

the Met Office Climate Science for Service Partnership (CSSP) China as part of the Newton Fund. CQ, JW, SD and HY were funded by the National Key R&D Program of China (2016YFA0600400), CCSF201704, CAS International Collaboration Program (2016), the NSFC (41675074, 41675093, 41301041), the Youth Innovation Promotion Association CAS (2016075), and the Jiangsu Collaborative Innovation Center for Climate Change.

REFERENCES

- Burke, C., and P. Stott, 2017: Impact of anthropogenic climate change on the East Asian summer monsoon. *J. Climate*, **30**, 5205–5220, doi:10.1175/JCLI-D-16-0892.1.
- Cheung, H. H. N., W. Zhou, M. Y. T. Leung, C. M. Shun, S. M. Lee, and H. W. Tong, 2016: A strong phase reversal of the Arctic Oscillation in midwinter 2015/2016: Role of the stratospheric polar vortex and tropospheric blocking. *J. Geophys. Res. Atmos.*, **121**, 13,443–13,457, doi:10.1002/2016JD025288.
- Christidis, N., P. A. Stott, A. A. Scaife, A. Arribas, G. S. Jones, D. Copsey, J. R. Knight, and W. J. Tennant, 2013: A new HadGEM3-A-based system for attribution of weather- and climate-related extreme events. *J. Climate*, **26**, 2756–2783, doi:10.1175/JCLI-D-12-00169.1.
- CMA, 2017: China Climate Bulletin 2016. China Meteorological Administration.
- Francis, J. A., and S. J. Vavrus, 2015: Evidence for a wavier jet stream in response to rapid Arctic warming. *Environ. Res. Lett.*, **10**, 014005, doi:10.1088/1748-9326/10/1/014005.
- Kug, J.-S., J.-H. Jeong, Y.-S. Jang, B.-M. Kim, C. K. Folland, S.-K. Min, and S.-W. Son, 2015: Two distinct influences of Arctic warming on cold winters over North America and East Asia. *Nat. Geosci.*, **8**, 759–762, doi:10.1038/ngeo2517.
- Li, Z., Z. W. Yan, and H. Y. Wu, 2015: Updated homogenized Chinese temperature series with physical consistency. *Atmos. Oceanic. Sci. Lett.*, **8**, 17–22, doi:10.3878/AOSL20140062.
- McCusker, K. E., J. C. Fyfe, and M. Sigmond, 2016: Twenty-five winters of unexpected Eurasian cooling unlikely due to Arctic sea-ice loss. *Nat. Geosci.*, **9**, 838–842, doi:10.1038/ngeo2820.
- Mori, M., M. Watanabe, H. Shiogama, J. Inoue, and M. Kimoto, 2014: Robust Arctic sea-ice influence on the frequent Eurasian cold winters in past decades. *Nat. Geosci.*, **7**, 869–873, doi:10.1038/NGEO2277.
- Pall, P., T. Aino, D. A. Stone, P. A. Stott, T. Nozawa, A. G. J. Hilberts, D. Lohmann, and M. R. Allen, 2011: Anthropogenic greenhouse gas contribution to flood risk in England and Wales in autumn 2000. *Nature*, **470**, 382–386, doi:10.1038/nature09762.
- Stott, P. A., D. A. Stone, and M. R. Allen, 2004: Human contribution to the European heatwave of 2003. *Nature*, **432**, 610–614, doi:10.1038/nature03089.
- , and Coauthors, 2016: Attribution of extreme weather and climate-related events. *Wiley Interdisc. Rev.: Climate Change*, **7**, 23–41, doi:10.1002/wcc.380.
- Sun, L., J. Perlwitz, and M. Hoerling, 2016: What caused the recent “warm Arctic, cold continents” trend pattern in winter temperatures? *Geophys. Res. Lett.*, **43**, 5345–5352, doi:10.1002/2016GL069024.
- Szentimrey, T., 1999: Multiple analyses of series for homogenization (MASH). *Proc. of the Second Seminar for Homogenization of Surface Climatological Data*, WMO-TD-962, Budapest, Hungary, WMO, 27–46.
- Trenary, L., T. DelSole, M. K. Tippett, and B. Doty, 2016: Extreme eastern U.S. winter of 2015 not symptomatic of climate change [in “Explaining Extreme Events of 2015 from a Climate Perspective”]. *Bull. Amer. Meteor. Soc.*, **97** (12), S31–S35, doi:10.1175/BAMS-D-16-0156.1.
- Walters, D., and Coauthors, 2017: The Met Office Unified Model Global Atmosphere 6.0/6.1 and JULES Global Land 6.0/6.1 configurations. *Geosci. Model Dev.*, **10**, 1487–1520, doi:10.5194/gmd-10-1487-2017.
- Wang, X. L., and V. R. Swail, 2001: Changes of extreme wave heights in Northern Hemisphere oceans and related atmospheric circulation regimes. *J. Climate*, **14**, 2204–2221, doi:10.1175/1520-0442(2001)014<2204:COEWHI>2.0.CO;2.

Table I.I. SUMMARY of RESULTS

ANTHROPOGENIC INFLUENCE ON EVENT			
	INCREASE	DECREASE	NOT FOUND OR UNCERTAIN
Heat	Ch. 3: Global Ch. 7: Arctic Ch. 15: France Ch. 19: Asia		
Cold		Ch. 23: China Ch. 24: China	
Heat & Dryness	Ch. 25: Thailand		
Marine Heat	Ch. 4: Central Equatorial Pacific Ch. 5: Central Equatorial Pacific Ch. 6: Pacific Northwest Ch. 8: North Pacific Ocean/Alaska Ch. 9: North Pacific Ocean/Alaska Ch. 9: Australia		Ch. 4: Eastern Equatorial Pacific
Heavy Precipitation	Ch. 20: South China Ch. 21: China (Wuhan) Ch. 22: China (Yangtze River)		Ch. 10: California (failed rains) Ch. 26: Australia Ch. 27: Australia
Frost	Ch. 29: Australia		
Winter Storm			Ch. 11: Mid-Atlantic U.S. Storm "Jonas"
Drought	Ch. 17: Southern Africa Ch. 18: Southern Africa		Ch. 13: Brazil
Atmospheric Circulation			Ch. 15: Europe
Stagnant Air			Ch. 14: Western Europe
Wildfires	Ch. 12: Canada & Australia (Vapor Pressure Deficits)		
Coral Bleaching	Ch. 5: Central Equatorial Pacific Ch. 28: Great Barrier Reef		
Ecosystem Function		Ch. 5: Central Equatorial Pacific (Chl- a and primary production, sea bird abundance, reef fish abundance) Ch. 18: Southern Africa (Crop Yields)	
El Niño	Ch. 18: Southern Africa		Ch. 4: Equatorial Pacific (Amplitude)
TOTAL	18	3	9

METHOD USED			Total Events
Heat	Ch. 3: CMIP5 multimodel coupled model assessment with piCont, historicalNat, and historical forcings Ch. 7: CMIP5 multimodel coupled model assessment with piCont, historicalNat, and historical forcings Ch. 15: Flow analogues conditional on circulation types Ch. 19: MIROC-AGCM atmosphere only model conditioned on SST patterns		
Cold	Ch. 23: HadGEM3-A (GA6) atmosphere only model conditioned on SST and SIC for 2016 and data fitted to GEV distribution Ch. 24: CMIP5 multimodel coupled model assessment		
Heat & Dryness	Ch. 25: HadGEM3-A N216 Atmosphere only model conditioned on SST patterns		
Marine Heat	Ch. 4: SST observations; SGS and GEV distributions; modeling with LIM and CGCMs (NCAR CESM-LE and GFDL FLOR-FA) Ch. 5: Observational extrapolation (OISST, HadISST, ERSST v4) Ch. 6: Observational extrapolation; CMIP5 multimodel coupled model assessment Ch. 8: Observational extrapolation; CMIP5 multimodel coupled model assessment Ch. 9: Observational extrapolation; CMIP5 multimodel coupled model assessment		
Heavy Precipitation	Ch. 10: CAM5 AMIP atmosphere only model conditioned on SST patterns and CESM1 CMIP single coupled model assessment Ch. 20: Observational extrapolation; CMIP5 and CESM multimodel coupled model assessment; auto-regressive models Ch. 21: Observational extrapolation; HadGEM3-A atmosphere only model conditioned on SST patterns; CMIP5 multimodel coupled model assessment with ROF Ch. 22: Observational extrapolation, CMIP5 multimodel coupled model assessment Ch. 26: BoM seasonal forecast attribution system and seasonal forecasts Ch. 27: CMIP5 multimodel coupled model assessment		
Frost	Ch. 29: <i>weather@home</i> multimodel atmosphere only models conditioned on SST patterns; BoM seasonal forecast attribution system		
Winter Storm	Ch. 11: ECHAM5 atmosphere only model conditioned on SST patterns		
Drought	Ch. 13: Observational extrapolation; <i>weather@home</i> multimodel atmosphere only models conditioned on SST patterns; HadGEM3-A and CMIP5 multimodel coupled model assessment; hydrological modeling Ch. 17: Observational extrapolation; CMIP5 multimodel coupled model assessment; VIC land surface hydrological model, optimal fingerprint method Ch. 18: Observational extrapolation; <i>weather@home</i> multimodel atmosphere only models conditioned on SSTs, CMIP5 multimodel coupled model assessment		
Atmospheric Circulation	Ch. 15: Flow analogues distances analysis conditioned on circulation types		
Stagnant Air	Ch. 14: Observational extrapolation; Multimodel atmosphere only models conditioned on SST patterns including: HadGEM3-A model; EURO-CORDEX ensemble; EC-EARTH+RACMO ensemble		
Wildfires	Ch. 12: HadAM3 atmosphere only model conditioned on SSTs and SIC for 2015/16		
Coral Bleaching	Ch. 5: Observations from NOAA Pacific Reef Assessment and Monitoring Program surveys Ch. 28: CMIP5 multimodel coupled model assessment; Observations of climatic and environmental conditions (NASA GES DISC, HadCRUT4, NOAA OISSTV2)		
Ecosystem Function	Ch. 5: Observations of reef fish from NOAA Pacific Reef Assessment and Monitoring Program surveys; visual observations of seabirds from USFWS surveys. Ch. 18: Empirical yield/rainfall model		
El Niño	Ch. 4: SST observations; SGS and GEV distributions; modeling with LIM and CGCMs (NCAR CESM-LE and GFDL FLOR-FA) Ch. 18: Observational extrapolation; <i>weather@home</i> multimodel atmosphere only models conditioned on SSTs, CMIP5 multimodel coupled model assessment		
			30